







Short Note

# 2,7-Bis(pyridin-3-ylethynyl)fluoren-9-one

Enrico Podda <sup>1,2,\*</sup> , Massimiliano Arca <sup>1</sup> , Anna Pintus <sup>1</sup> , Valentina Demontis <sup>1</sup>, Vito Lippolis <sup>1</sup> , Giulio Ferino <sup>2</sup> , James B. Orton <sup>3</sup>, Simon J. Coles <sup>3</sup> and Maria Carla Aragoni <sup>1,\*</sup> 

<sup>1</sup> Department of Chemical and Geological Sciences, University of Cagliari, Cittadella Universitaria, S.S. 554 bivio Sestu, Monserrato, 09042 Cagliari, Italy

<sup>2</sup> Centre for Research University Services (CeSAR), University of Cagliari, Cittadella Universitaria, S.S. 554 bivio Sestu, Monserrato, 09042 Cagliari, Italy

<sup>3</sup> UK National Crystallography Service, School of Chemistry, Faculty of Engineering and Physical Sciences, University of Southampton, Southampton SO17 1BJ, UK

\* Correspondence: enrico.podda@unica.it (E.P.); aragoni@unica.it (M.C.A.)

**Abstract:** 2,7-bis(pyridin-3-ylethynyl)fluoren-9-one [(3-PyE)<sub>2</sub>FO] was synthesized in one step by the Sonogashira coupling reaction between 3-ethynylpyridine and 2,7-dibromofluoren-9-one. The title compound was fully characterized, and its crystal structure was determined through single-crystal XRD analysis.

**Keywords:** fluoren-9-one; polypyridyl donors; luminescence; SC-XRD

## 1. Introduction

The construction of novel supramolecular architectures and functional materials starts with the design of appropriate building blocks with determined functional and geometrical properties [1]. Organic linkers, including fluorophores in their skeletons, can be designed to impart peculiar luminescence properties to the final supramolecular networks. Fluorene and their oxidized fluorenone derivatives have been employed to develop new materials that are very promising for photonic and optoelectronic applications, such as optical second harmonic (SGH) and terahertz (THz) generation, light emitting diodes, biomarkers, solar cells, and sensors [2–4]. During recent decades, discrete fluorene-based building blocks have been extensively studied, featuring either a single fluorene [5] or fluorenone [6] moiety or multiple fluorene cores, such as spirobifluorene [7] and cofacial bifluorene derivatives [8].

Most fluorenone derivatives recently reported in the literature, such as 2,7-diphenylfluoren-9-one [(Ph)<sub>2</sub>FO] [9], 2,7-di([1,1'-biphenyl]-4-yl)fluoren-9-one [(4-BPy)<sub>2</sub>FO] [10], and 2,7-bis(phenylethynyl)fluoren-9-one [(PhE)<sub>2</sub>FO] [11] (Figure 1), do not feature donor sites suitable for metal coordination and find applications only for the preparation of purely organic materials. To overcome this limitation and extend their use to the fabrication of hybrid metal-organic frameworks, fluorenone carboxylate derivatives can be prepared by including charged donor sites in the structure, such as fluoren-9-one-2,7-dicarboxylate [12]. Neutral supramolecular spacers can also be prepared by exploiting neutral donor sites, such as pyridyl groups; see, for example, 2,7-di(pyridin-3-yl)fluoren-9-one [(3-Py)<sub>2</sub>FO] [6], 2,7-di(pyridin-4-yl)fluoren-9-one [(4-Py)<sub>2</sub>FO] [13–15] and (2,7-bis(2-(pyridin-3-yl)vinyloxy)fluoren-9-one [(4-PyV)<sub>2</sub>FO] [16] (Figure 1). Apart from these few examples, the design of pyridyl-functionalized fluorenone derivatives is still largely unexplored. Here, we report the synthesis and full characterization of the novel pyridyl-functionalized fluorenone 2,7-bis(pyridin-3-ylethynyl)fluoren-9-one [(3-PyE)<sub>2</sub>FO] (Scheme 1).



**Citation:** Podda, E.; Arca, M.; Pintus, A.; Demontis, V.; Lippolis, V.; Ferino, G.; Orton, J.B.; Coles, S.J.; Aragoni, M.C. 2,7-Bis(pyridin-3-ylethynyl)fluoren-9-one. *Molbank* **2023**, *2023*, M1540. <https://doi.org/10.3390/M1540>

Academic Editor: Kristof Van Hecke

Received: 19 December 2022

Revised: 2 January 2023

Accepted: 3 January 2023

Published: 9 January 2023



**Copyright:** © 2023 by the authors. Licensee MDPI, Basel, Switzerland. This article is an open access article distributed under the terms and conditions of the Creative Commons Attribution (CC BY) license (<https://creativecommons.org/licenses/by/4.0/>).

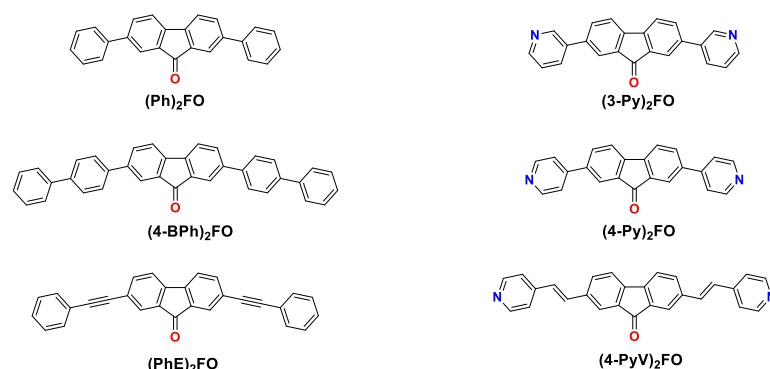
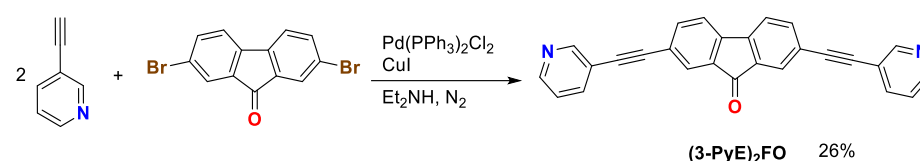


**Figure 1.** Selected fluorenone-based building blocks: [(Ph)<sub>2</sub>FO] [9]; [(3-Py)<sub>2</sub>FO] [6]; [(4-BPh)<sub>2</sub>FO] [10]; [(4-Py)<sub>2</sub>FO] [13–15]; [(PhE)<sub>2</sub>FO] [11]; [(4-PyV)<sub>2</sub>FO] [16].



**Scheme 1.** Synthesis of 2,7-bis(pyridin-3-ylethynyl)fluoren-9-one [(3-PyE)<sub>2</sub>FO].

## 2. Results and Discussion

Compound (3-PyE)<sub>2</sub>FO was synthesized by adapting a procedure previously reported for the preparation of 2,5-bis(pyridin-3-ylethynyl)thiophene [17]. Two equivalents of 3-ethynylpyridine were reacted with 2,7-dibromofluorenone in dry diethylamine under inert atmosphere by following a classical Pd/Cu-catalyzed tandem Sonogashira coupling reaction (Scheme 1) [18].

The crude product was recrystallized to give pure (3-PyE)<sub>2</sub>FO as light-orange crystals with a 26% yield. FTIR analysis showed the stretching modes of alkynyl and carbonyl moieties at 2206 and 1716 cm<sup>-1</sup>, respectively, with <sup>1</sup>H and <sup>13</sup>C{<sup>1</sup>H} NMR spectra in agreement with the chemical structure of (3-PyE)<sub>2</sub>FO. The absorption and emission properties of (3-PyE)<sub>2</sub>FO were investigated in solution and in the solid state (Figure 2). The UV-Vis spectrum of (3-PyE)<sub>2</sub>FO in CHCl<sub>3</sub> exhibited four maxima centered at 304, 339, 349, and 436 nm, and a photoluminescence emission was observed at 554 nm ( $\Phi = 0.04$ ,  $\lambda_{\text{ex}} = 350$  nm). Solid-state measurements showed a broad absorption in the diffuse reflectance spectrum in the range of 200–500 nm and a strong emission band of 553 nm, similar to what was observed in solution.

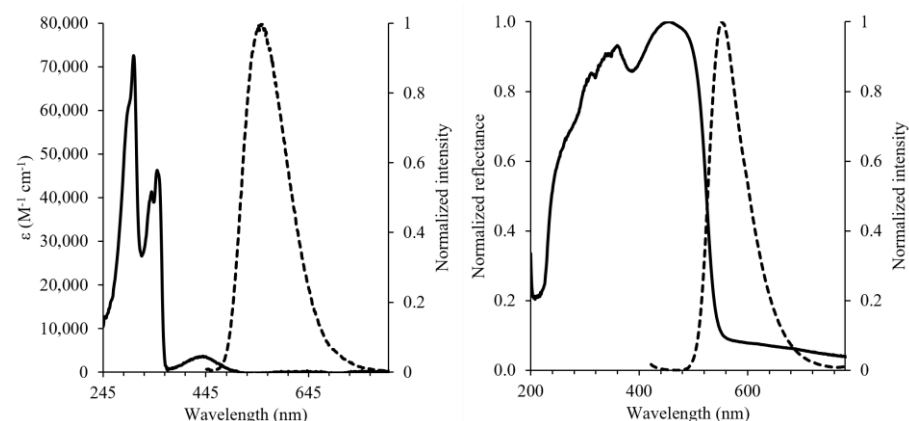


**Figure 2.** Absorption (solid line) and photoluminescence emission (dashed line) spectra for (3-PyE)<sub>2</sub>FO measured in CHCl<sub>3</sub> (left) ( $C = 10^{-5}$ – $10^{-6}$  M,  $\lambda_{\text{ex}} = 350$  nm) and in the solid state (right) ( $\lambda_{\text{ex}} = 400$  nm).

A crystal suitable for X-ray diffraction analysis was selected and structurally characterized. The compound  $(3\text{-PyE})_2\text{FO}$  crystallized in the monoclinic space group  $P2_1/c$  with a single molecule in the asymmetric unit, as shown in Figure 3. The compound adopted an almost planar geometry with one pyridyl ring coplanar with the fluorenone ring (torsion angle  $\simeq 1^\circ$ ), and the other twisted with respect to the fluorenone plane by about  $33^\circ$ .

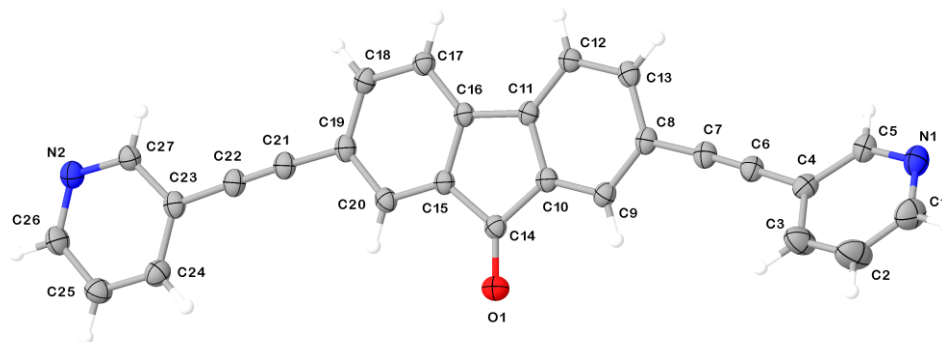


**Figure 3.** Ellipsoid plot of  $(3\text{-PyE})_2\text{FO}$  with the numbering scheme adopted. Displacement ellipsoids are drawn at 50% probability level.

Crystal data for  $(3\text{-PyE})_2\text{FO}$ :  $\text{C}_{27}\text{H}_{14}\text{N}_2\text{O}$  ( $M_r = 382.40 \text{ g mol}^{-1}$ ), monoclinic,  $P2_1/c$  (No. 14),  $a = 6.6190(1) \text{ \AA}$ ,  $b = 13.7115(1) \text{ \AA}$ ,  $c = 22.1683(3) \text{ \AA}$ ,  $\beta = 110.080(1)^\circ$ ,  $\alpha = \gamma = 90^\circ$ ,  $V = 1889.62(4) \text{ \AA}^3$ ,  $T = 100(2) \text{ K}$ ,  $Z = 4$ ,  $Z' = 1$ ,  $\mu(\text{Cu K}\alpha) = 0.653$ . A total of 57,856 reflections were measured, and 3441 unique reflections ( $R_{int} = 0.0247$ ) were used in all calculations. The final  $wR_2$  was 0.1204 (all data), and  $R_1$  was 0.0455 ( $I \geq 2 \sigma(I)$ ).

A full interaction map [19] was calculated for this structure (based on pre-extracted IsoStar interaction data from the CSD), which implies that crystal packing was driven by a combination  $\pi$ - $\pi$  interactions and  $\text{CH}\cdots\text{O}$  and  $\text{CH}\cdots\text{N}$  hydrogen bonds (Figure S1, Supplementary Materials). Adjacent molecules of  $(3\text{-PyE})_2\text{FO}$  are pillared along the  $a$ -axis through intermolecular  $\pi$ - $\pi$  interactions between fluorenone and pyridyl moieties (3.66–3.81  $\text{\AA}$ , Figure 4a and Figure S1). Molecules located on vicinal pillars are rotated by about  $61^\circ$ , generating a zig-zag packing motif (Figure 4b), strongly resembling that found in the  $\alpha$ -phase of  $(\text{PhE})_2\text{FO}$  [11].

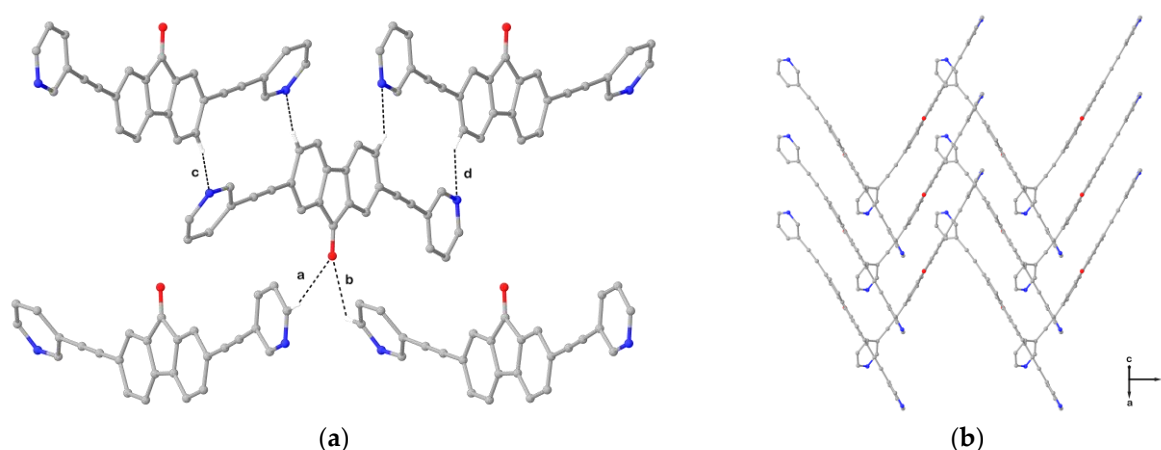


**Figure 4.** Packing diagrams of  $(3\text{-PyE})_2\text{FO}$  showing hydrogen bonding network along the  $a$ -axis (a) and the zig-zag packing motif along the (101) direction (b). Interactions are labeled according to Table S1.

The presence of the oxygen and nitrogen atoms in  $(3\text{-PyE})_2\text{FO}$  promotes, respectively, the formation of two weak  $\text{CH}\cdots\text{O}$  hydrogen bonds with *para*-positioned hydrogen atoms of pyridyl rings (interactions  $a$  and  $b$  in Figure 4a) belonging to two molecule units located on the adjacent pillars and two  $\text{CH}\cdots\text{N}$  hydrogen bonds involving hydrogen atoms located at the fluorenone core (interactions  $c$  and  $d$  in Figure 4a; see Table S1 for details).

### 3. Materials and Methods

#### 3.1. General

Solvents and reagents were purchased from TCI, FluoroChem, and Aldrich. Diethylamine was distilled over  $\text{LiAlH}_4$  and degassed prior to use. Syntheses were carried out under dry dinitrogen atmosphere using standard Schlenk equipment. FT-IR measurements were recorded at room temperature on a Thermo-Nicolet 5700 spectrometer using KBr pellets with a KBr beam splitter and KBr windows ( $4000\text{--}400\text{ cm}^{-1}$ , resolution  $4\text{ cm}^{-1}$ ). NMR spectra were carried out in  $\text{CDCl}_3$  at room temperature using a Bruker Avance III HD 600 spectrometer. Chemical shifts are reported in ppm ( $\delta$ ) and were calibrated to the solvent residue. Coupling constants  $J$  are reported in hertz (Hz). Positive ESI-MS spectra were recorded with a high-resolution LTQ Orbitrap Elite™ mass spectrometer (Thermo Fisher Scientific, Waltham, MA, USA). The solutions were infused at a flow rate of  $5.00\text{ }\mu\text{L}/\text{min}$  into the ESI source. Spectra were recorded in the range of  $m/z$  300–600 with a resolution of 240,000 (FWHM). The instrumental conditions were as follows: a spray voltage of 3500 V, a capillary temperature of  $275\text{ }^\circ\text{C}$ , sheath gas 12 (arbitrary units), auxiliary gas 3 (arbitrary units), sweep gas 0 (arbitrary units), and a probe heater temperature of  $50\text{ }^\circ\text{C}$ . Elemental analysis was carried out with a CHNS/O PE 2400 series II elemental analyzer ( $T = 925\text{ }^\circ\text{C}$ ). The melting point was determined on a FALC mod. C (up to  $290\text{ }^\circ\text{C}$ ) apparatus. UV-Vis measurements in solution were recorded in the range of 190–1100 nm using quartz cuvettes with a path length of 1.0 cm by means of an Agilent Cary 5000 UV–vis–NIR dual-beam spectrophotometer. Diffuse reflectance measurements were carried out on an Agilent Cary 5000 UV–vis–NIR dual-beam spectrophotometer equipped with a diffuse reflectance accessory. Photoluminescence emission spectra in solution and solid state were collected either on a Varian Cary Eclipse spectrofluorometer or a Perkin Elmer LS55 fluorescence spectrometer. The photoluminescence quantum yield  $\Phi$  was determined according to Equation (1) and using rhodamine 6G as a standard ( $\Phi_{\text{ST}} = 0.95$  in ethanol) [20].

$$\Phi_X = \Phi_{\text{ST}} \left( \frac{\text{Grad}_X}{\text{Grad}_{\text{ST}}} \right) \left( \frac{\eta_X^2}{\eta_{\text{ST}}^2} \right) \quad (1)$$

where the subscripts ST and X denote standard and sample, respectively; Grad is the gradient from the plot of integrated fluorescence intensity vs. absorbance; and  $\eta$  is the refractive index of the solvent.

X-ray diffraction data for **(3-PyE)<sub>2</sub>FO** were collected at 100 (2) K on a Rigaku 007HF diffractometer equipped with Varimax confocal mirrors, an AFC11 goniometer, and a HyPix 6000 detector. The structure was solved with the ShelXT [21] solution program using dual methods, and the model was refined with ShelXL 2018/3 [22] using full-matrix least-squares minimization on  $F^2$ . Olex2 1.5 [23] was used as the graphical interface.

#### 3.2. Synthesis of 2,7-Bis(pyridin-3-ylethynyl)fluoren-9-one [(3-PyE)<sub>2</sub>FO]

3-Ethynylpyridine (517 mg; 5.0 mmol), 2,7-dibromofluoren-9-one (845 mg; 2.5 mmol), copper iodide (24 mg; 0.13 mmol), and  $\text{Pd}(\text{PPh}_3)_2\text{Cl}_2$  (90 mg; 0.13 mmol) were dried under vacuum for 20 min, and freshly distilled and degassed diethylamine (25 mL) was added under dry  $\text{N}_2$  atmosphere. The yellow mixture was heated to  $55\text{ }^\circ\text{C}$  and stirred under inert atmosphere for 24 h. The mixture slowly turned red in 30 min, and the day after, an intense yellow color was observed. After cooling to RT, a  $\text{NH}_4\text{Cl}$  saturated aqueous solution (100 mL) was added, and the precipitate was separated by filtration under vacuum. The crude yellow product was recrystallized from the DCM/EtOAc mixture to yield the title compound as light-orange crystals (230 mg; 0.60 mmol;  $Y = 24\%$ ). M. p. =  $249\text{ }^\circ\text{C}$ . ESI (+)-MS (MeCN solution)  $m/z$  383.1195 for  $[\text{C}_{27}\text{H}_{15}\text{N}_2\text{O}]^+ [\text{M}-\text{H}]^+$ . Elemental analysis calculated (%) for  $\text{C}_{27}\text{H}_{14}\text{N}_2\text{O}$ : C 84.80, H 3.69, N 7.33. Found: C 84.20, H 3.45, N 7.21. FTIR (KBr,  $4000\text{--}400\text{ cm}^{-1}$ ): 3053 w, 3035 w, 3003 w, 2206 w  $\nu\text{C}\equiv\text{C}$ , 1959 w, 1928 w, 1896 w, 1863 w, 1807 w, 1782 w, 1716 s, 1614 ms, 1604 ms, 1581 mw, 1556 m, 1479 vs, 1464 ms, 1427 m, 1400 ms, 1385 w, 1315 m, 1245 m, 1209 w, 1194 m, 1186 m, 1115 m, 1020 m, 1014 m,

982 mw, 949 w, 922 w, 902 mw, 831 m, 833 ms, 802 ms, 783 s, 735 w, 702 s, 650 m, 623 m, 578 w, 540 m, 515 mw, 473 w, 428 w, 405 mw cm<sup>-1</sup>. <sup>1</sup>H NMR (600 MHz, CDCl<sub>3</sub>) δ: 8.78 (d, J = 1.4 Hz, 2H), 8.58 (dd, J = 4.9, 1.6 Hz, 2H), 7.86–7.82 (m, 4H), 7.70 (dd, J = 7.7, 1.4 Hz, 2H), 7.57 (d, J = 7.7 Hz, 2H), 7.33 (dd, J = 7.7, 4.9 Hz, 2H) ppm. <sup>13</sup>C{<sup>1</sup>H} NMR (151 MHz, CDCl<sub>3</sub>) δ: 192.0, 152.2, 148.9, 143.7, 138.9, 138.1, 134.7, 127.7, 124.0, 123.3, 120.9, 120.2, 91.9, 88.1 ppm.

#### 4. Conclusions

The novel visible-emitting fluorophore 2,7-bis(pyridin-3-ylethynyl)fluoren-9-one [(3-PyE)<sub>2</sub>FO] was successfully prepared by the Sonogashira coupling reaction, and its full characterization was presented. Further studies are ongoing in our laboratories to evaluate the potential use of (3-PyE)<sub>2</sub>FO as a building block for the formation of luminescent supramolecular assemblies.

**Supplementary Materials:** Figure S1: Interaction maps; Figures S2 and S3: <sup>1</sup>H and <sup>13</sup>C{<sup>1</sup>H} NMR spectra; Figure S4: FTIR spectrum; Figure S5: ESI (+) MS spectrum; Table S1: Hydrogen bonding; Table S2: Crystal data and refinement parameters; Tables S3 and S4: Bond lengths and angles.

**Author Contributions:** Conceptualization, M.C.A. and E.P.; data curation, M.C.A., E.P., A.P., M.A., J.B.O. and S.J.C.; investigation, M.C.A., E.P., V.D., M.A., V.L., G.F., S.J.C., J.B.O. and A.P.; writing (original draft), M.C.A. and E.P. All authors have read and agreed to the published version of the manuscript.

**Funding:** The authors acknowledge Fondazione di Sardegna (FdS Progetti Biennali di Ateneo, annualità 2018) for financial support.

**Data Availability Statement:** Crystallographic data were deposited at CCCD (CIF deposition number 2225299).

**Acknowledgments:** CeSAR (Center for Research University Services of the University of Cagliari is kindly acknowledged for NMR and MS facilities.

**Conflicts of Interest:** The authors declare no conflict of interest.

#### References

1. Albano, V.G.; Aragoni, M.C.; Arca, M.; Castellari, C.; Demartin, F.; Devillanova, F.A.; Isaia, F.; Lippolis, V.; Loddo, L.; Verani, G. An unprecedented example of a *cis*-phosphonodithioato nickel(ii) complex built by an extensive hydrogen bonding supramolecular network. *Chem. Commun.* **2002**, *11*, 1170–1171. [[CrossRef](#)] [[PubMed](#)]
2. Semin, S.; Li, X.; Duan, Y.; Rasing, T.; Semin, S.; Li, X.; Duan, Y.; Rasing, T. Nonlinear Optical Properties and Applications of Fluorenone Molecular Materials. *Adv. Opt. Mater.* **2021**, *9*, 2100327. [[CrossRef](#)]
3. Liu, B.; Yu, W.L.; Lai, Y.H.; Huang, W. Blue-Light-Emitting Fluorene-Based Polymers with Tunable Electronic Properties. *Chem. Mater.* **2001**, *13*, 1984–1991. [[CrossRef](#)]
4. Gong, X.; Iyer, P.K.; Moses, D.; Bazan, G.C.; Heeger, A.J.; Xiao, S.S. Stabilized Blue Emission from Polyfluorene-Based Light-Emitting Diodes: Elimination of Fluorenone Defects. *Adv. Funct. Mater.* **2003**, *13*, 325–330. [[CrossRef](#)]
5. Guo, H.D.; Guo, X.M.; Batten, S.R.; Song, J.F.; Song, S.Y.; Dang, S.; Zheng, G.L.; Tang, J.K.; Zhang, H.J. Hydrothermal Synthesis, Structures, and Luminescent Properties of Seven d<sup>10</sup> Metal-Organic Frameworks Based on 9,9-Dipropylfluorene-2,7-Dicarboxylic Acid (H<sub>2</sub>DFDA). *Cryst. Growth Des.* **2009**, *9*, 1394–1401. [[CrossRef](#)]
6. Tessarolo, J.; Lee, H.; Sakuda, E.; Umakoshi, K.; Clever, G.H. Integrative Assembly of Heteroleptic Tetrahedra Controlled by Backbone Steric Bulk. *J. Am. Chem. Soc.* **2021**, *143*, 6339–6344. [[CrossRef](#)]
7. Moreau, F.; Audebrand, N.; Poriel, C. 9,9'-Spirofluorene Based Zinc Coordination Polymers: A Study on Linker Geometry and Topology. *CrystEngComm* **2019**, *22*, 293–303. [[CrossRef](#)]
8. Podda, E.; Arca, M.; Pintus, A.; Lippolis, V.; Caltagirone, C.; Coles, S.J.; Orton, J.B.; Ennas, G.; Picci, G.; Davies, R.P.; et al. On the role of torsional dynamics in the solid-state fluorescent properties of a new bifluorene-tetracarboxylic acid and its supramolecular assemblies: A structural and DFT investigation. *CrystEngComm* **2023**, submitted.
9. Xu, J.; Semin, S.; Niedzialek, D.; Kouwer, P.H.; Fron, E.; Coutino, E.; Savoini, M.; Li, Y.; Hofkens, J.; Uji-I, H.; et al. Self-Assembled Organic Microfibers for Nonlinear Optics. *Adv. Mater.* **2013**, *25*, 2084–2089. [[CrossRef](#)]
10. Duan, Y.; Ju, C.; Yang, G.; Fron, E.; Coutino-Gonzalez, E.; Semin, S.; Fan, C.; Balok, R.S.; Cremers, J.; Tinnemans, P.; et al. Aggregation Induced Enhancement of Linear and Nonlinear Optical Emission from a Hexaphenylene Derivative. *Adv. Funct. Mater.* **2016**, *26*, 8968–8977. [[CrossRef](#)]
11. Li, X.; Semin, S.; Estrada, L.A.; Yuan, C.; Duan, Y.; Cremers, J.; Tinnemans, P.; Kouwer, P.; Rowan, A.E.; Rasing, T.; et al. Strong Optical Nonlinearities of Self-Assembled Polymorphic Microstructures of Phenylethynyl Functionalized Fluorenones. *Chin. Chem. Lett.* **2018**, *29*, 297–300. [[CrossRef](#)]

12. See Refcodes: AXOVEP, AXOVIT, COJMIZ, HACNIL, LINZUG, MACHIJ, NOMLIM, PEKCOA, SOQSAU, TOHQUE, TOWNIE, UQIVIB, ZUFZIJ. Crystal Structures Can be Accessed/Downloaded for Free from. Available online: <https://www.ccdc.cam.ac.uk/structures/> (accessed on 1 January 2023).
13. Wang, J.; Cheng, Y.; Zhou, J.; Tang, W. A Donor-Acceptor Liganded Metal-Organic Framework Showcases the Hydrogen-Bond-Enhanced Sensing of N-Heterocyclic Explosives. *J. Mater. Chem. C Mater.* **2021**, *9*, 12086–12093. [[CrossRef](#)]
14. Liu, Z.; Wang, M.; Chen, K.; Liu, B.; Wang, D.; You, Y.; Zhou, X.; Huang, W. Syntheses, Structures, and Properties of Four Coordination Polymers Based on 2,7-Di(Pyridin-4-yl)-9H-Fluoren-9-One. *Appl. Organomet Chem.* **2020**, *34*, e5477. [[CrossRef](#)]
15. Tan, Y.; Wang, Z.K.; Lang, F.F.; Yu, H.M.; Cao, C.; Ni, C.Y.; Wang, M.Y.; Song, Y.L.; Lang, J.P. Construction of Cluster-Based Supramolecular Wire and Rectangle. *Dalton Trans.* **2022**, *51*, 6358–6365. [[CrossRef](#)]
16. Behrendt, A.; Couchman, S.M.; Jeffery, J.C.; McCleverty, J.A.; Ward, M.D. Complexes Containing Redox-Active Fluorenone-Based Ligands Linked to Redox-Active Tris(Pyrazolyl)Boratomolybdenum Fragments: Assignment of Ligand-Centred and Metal-Centred Redox Processes by EPR and UV/VIS/NIR Spectroelectrochemistry<sup>†</sup>. *J. Chem. Soc. Dalton Trans.* **1999**, *24*, 4349–4355. [[CrossRef](#)]
17. Podda, E.; Coles, S.J.; Horton, P.N.; Lickiss, P.D.; Bull, O.S.; Orton, J.B.; Pintus, A.; Pugh, D.; Carla Aragoni, M.; Davies, R.P. First Example of Solid-State Luminescent Borasiloxane-Based Chiral Helices Assembled through N–B Bonds. *Dalton Trans.* **2021**, *50*, 3782–3785. [[CrossRef](#)]
18. Tykwinski, R.R. Evolution in the Palladium-Catalyzed Cross-Coupling of sp- and sp<sup>2</sup>-Hybridized Carbon Atoms. *Angew. Chem. Int. Ed.* **2003**, *42*, 1566–1568. [[CrossRef](#)]
19. Wood, P.A.; Olsson, T.S.G.; Cole, J.C.; Cottrell, S.J.; Feeder, N.; Galek, P.T.A.; Groom, C.R.; Pidcock, E. Evaluation of Molecular Crystal Structures Using Full Interaction Maps. *CrystEngComm* **2012**, *15*, 65–72. [[CrossRef](#)]
20. Kubin, R.F.; Fletcher, A.N. Fluorescence quantum yields of some rhodamine dyes. *J. Lumin.* **1982**, *27*, 455–462. [[CrossRef](#)]
21. Sheldrick, G.M. SHELXT—Integrated Space-Group and Crystal-Structure Determination. *Acta. Cryst. A* **2015**, *71*, 3–8. [[CrossRef](#)]
22. Sheldrick, G.M. Crystal Structure Refinement with SHELXL. *Acta. Cryst. C* **2015**, *71*, 3–8. [[CrossRef](#)] [[PubMed](#)]
23. Dolomanov, O.V.; Bourhis, L.J.; Gildea, R.J.; Howard, J.A.K.; Puschmann, H. OLEX2: A Complete Structure Solution, Refinement and Analysis Program. *J. Appl. Cryst.* **2009**, *42*, 339–341. [[CrossRef](#)]

**Disclaimer/Publisher’s Note:** The statements, opinions and data contained in all publications are solely those of the individual author(s) and contributor(s) and not of MDPI and/or the editor(s). MDPI and/or the editor(s) disclaim responsibility for any injury to people or property resulting from any ideas, methods, instructions or products referred to in the content.